



**HAL**  
open science

## The impact of freshening on phytoplankton production in the Pacific Arctic Ocean

Pierre Coupel, Diana Ruiz-Pino, Marie-Alexandrine Sicre, J. F. Chen, S. H. Lee, N. Schiffrine, H. L. Li, Jean-Claude Gascard

► **To cite this version:**

Pierre Coupel, Diana Ruiz-Pino, Marie-Alexandrine Sicre, J. F. Chen, S. H. Lee, et al.. The impact of freshening on phytoplankton production in the Pacific Arctic Ocean. *Progress in Oceanography*, 2015, 131, pp.113-125. 10.1016/j.pocean.2014.12.003 . hal-01103453

**HAL Id: hal-01103453**

**<https://hal.sorbonne-universite.fr/hal-01103453>**

Submitted on 14 Jan 2015

**HAL** is a multi-disciplinary open access archive for the deposit and dissemination of scientific research documents, whether they are published or not. The documents may come from teaching and research institutions in France or abroad, or from public or private research centers.

L'archive ouverte pluridisciplinaire **HAL**, est destinée au dépôt et à la diffusion de documents scientifiques de niveau recherche, publiés ou non, émanant des établissements d'enseignement et de recherche français ou étrangers, des laboratoires publics ou privés.

# 1 The impact of Freshening on phytoplankton production in the 2 Pacific Arctic Ocean

3  
4 P. Coupel<sup>1,2</sup>, D. Ruiz-Pino<sup>2</sup>, M.A. Sicre<sup>2</sup>, J. F. Chen<sup>3</sup>, S. H. Lee<sup>4</sup>, N. Schiffrine<sup>1</sup>, H.L. Li<sup>3</sup>, J.C.  
5 Gascard<sup>2</sup>

6  
7 <sup>1</sup>Joint International U.Laval-CNRS Laboratory Takuvik, Québec-Océan, Département de Biologie, Université  
8 Laval, Québec, Québec G1V 0A6, Canada

9 <sup>2</sup>Sorbonne Universités (UPMC, Université Paris 06)-CNRS-IRD-MNHN, LOCEAN Laboratory, 4 place Jussieu,  
10 F-75005 Paris, France

11 <sup>3</sup>Laboratory of Marine Ecosystem and Biogeochemistry, Second Institute of Oceanography (SIO), State Oceanic  
12 Administration (SOA), Hangzhou 310012, China

13 <sup>4</sup>Department of Oceanography, Pusan National University, 30, Jangjeon-dong, Busan 609-735, South Korea  
14

15 Corresponding author: Pierre Coupel - Québec-Océan - Pavillon Alexandre-Vachon - Local 2078 - Université  
16 Laval - Québec (Québec) G1V 0A6 □ Canada.  
17 Pierre.Coupel@takuvik.ulaval.ca - (418) 656 2131 poste 6582  
18

19 **Keyword:** *Polar waters, primary production, chlorophyll, nitracline, freshening, ice edge,*  
20 *stratification, Arctic Ocean, Canada Basin, Chukchi shelf*  
21

## 22 Abstract

23 Since the 1990's, drastic melting of sea ice and continental ice in the Arctic region,  
24 triggered by global warming, has caused substantial freshening of the Arctic Ocean. While  
25 several studies attempted to quantify the magnitude of this freshening, its consequences on  
26 primary producers remain poorly documented. In this study, we evaluate the impact of the  
27 freshwater content (FWC) of the upper Arctic Ocean on phytoplankton across the Pacific  
28 sector, from the Bering Strait (65°N) to the North Pole (86°N), during summer 2008. We  
29 performed statistical analyses on the physical, biogeochemical and biological data acquired  
30 during the CHINARE 2008 cruise to investigate the effect of sea-ice melting on the Arctic  
31 phytoplankton. We found that the strong freshening observed in the Canada Basin had a  
32 negative impact on primary producers as a result of the deepening of the nitracline and the  
33 establishment of a subsurface chlorophyll maximum (SCM). In contrast, regions with lower  
34 freshening, such as the Chukchi shelf and the marginal ice zone (MIZ) over the Chukchi  
35 Borderland, exhibited a shallower nitracline sustaining relatively high primary production and  
36 biomass. Our results imply that the predicted increase freshening in future years will likely

37 cause the Arctic deep basin to become more oligotrophic because of weaker surface nutrient  
38 renewal from the subsurface ocean, despite higher light penetration.

39

## 40 **1. Introduction**

41 The recent unprecedented decline of Arctic sea-ice cover and ice thickness minimum  
42 recorded in September 2007 (Comiso et al., 2008; Perovich, 2011; Stroeve et al., 2011)  
43 attracted attention of the international scientific community. With the acceleration of ice  
44 melting, environmental factors that are important to primary producers have changed  
45 (Wassmann and Reigstad, 2011) with consequences for marine resources and the carbon cycle  
46 (Anderson et al., 2010; Bates et al., 2006; Cai et al., 2010; Longhurst, 1991). Among them,  
47 the decrease in salinity of the upper Arctic Ocean was particularly notable (Mauritzen, 2012).  
48 Freshening was mostly exceptional in the Canada Basin where the freshwater volume  
49 increased by 8500 km<sup>3</sup> over the last 10 years due to higher sea ice melting, river runoff and  
50 stronger Ekman pumping associated with the Beaufort Gyre (McPhee et al., 2009; Rabe et al.,  
51 2011). The predicted increase of sea-ice melting and river discharge in the coming years will  
52 most likely intensify freshening of the Arctic Ocean (Peterson et al., 2006; Yamamoto-Kawai  
53 et al., 2009). One consequence of enhanced freshening is the deepening of the nitracline and  
54 chlorophyll maximum, as recently reported by McLaughlin and Carmack (2010) in the  
55 interior Canada Basin. According to these authors, on the long-term increased stratification  
56 and stronger Ekman pumping would reduce winter nutrient renewal in the euphotic layer and  
57 summer primary production. In contrast, the shallow Chukchi shelf waters could become  
58 more productive because of a longer productive season (Arrigo et al., 2008; Pabi et al., 2008)  
59 and intensification of shelf-break upwellings (Carmack and Chapman, 2003; Lee and  
60 Whitley, 2004). Contrasted responses of phytoplankton inhabiting shelves and deep basins  
61 were found by modeling results of cyclone activity in the Pacific Arctic using a coupled  
62 biophysical model (Zhang et al., 2014). A biological gain was observed over the shelf while  
63 the deep basin showed a loss. However, Yun et al. (2014) showed that in 2009 primary  
64 production in the Chukchi shelf waters was negatively affected by freshwater accumulation  
65 from Siberian Coastal Current. These results underline that the response of phytoplankton to  
66 environmental changes differs spatially owing to bathymetry, sea-ice dynamics, freshwater  
67 accumulation and nutrient availability (Ardyna et al., 2011; Carmack and Wassmann, 2006;  
68 Poulin et al., 2010). Whether primary production in the shelves and deep basin waters will  
69 increase or decrease as a result of ongoing changes in Arctic is still being debated. In this  
70 study, we investigate the effects of freshening on chlorophyll-*a* distribution and primary

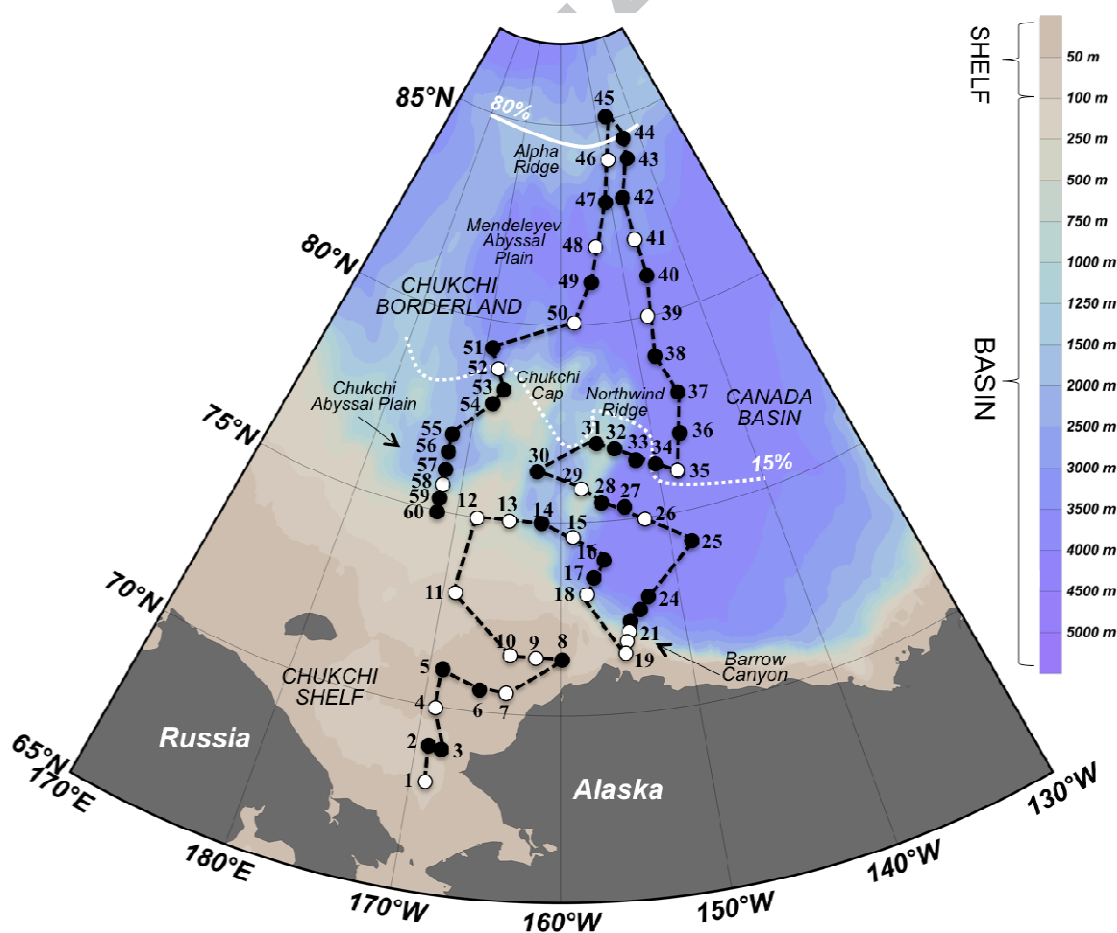
71 production in the Pacific Arctic Ocean in summer 2008. Biological, chemical and physical  
 72 data were acquired in a wide area from the Chukchi shelf to the central Arctic, encompassing  
 73 the Canada Basin and the Chukchi Borderland. This research work is part of the Chinese  
 74 National Arctic Research Expedition (CHINARE) program, undertaken aboard the icebreaker  
 75 *Xuelong*.

76

## 77 2. Material and Methods

### 78 2.1. The CHINARE 2008 cruise

79 The CHINARE 2008 cruise (1<sup>st</sup> August–8<sup>th</sup> September 2008) took place one year after  
 80 the large decline of the summer sea-ice cover in 2007 (Perovich et al., 2008; Stroeve et al.,  
 81 2011). The study area, extending from 65°N to 86°N, includes the shallow Chukchi shelf  
 82 (depth < 100 m) and deep basins (depth > 100 m). The ship track encompasses the Chukchi  
 83 Shelf, Barrow Canyon, Canada Basin, Northwind Ridge and the Alpha Ridge sampled in  
 84 August 2008, while the Mendeleev Abyssal Plain, Chukchi Cap and Chukchi Abyssal Plain  
 85 were sampled on the way back in September 2008 (Fig. 1).



86

87 *Figure 1. Station number occupied during the CHINARE 2008 cruise aboard the icebreaker*  
 88 *XueLong, from August 1<sup>rst</sup> to September 8<sup>th</sup>, 2008. Stations where nutrients and chlorophyll-a*  
 89 *(Chla) were both measured are indicated by black and white dots. Stations where primary*  
 90 *production (PP) was also measured are shown by the white dots. The black dashed line*  
 91 *represents the ship track. The color scale features the bathymetry and distinguishes the shelf*  
 92 *(< 100 m) from the deep basins (> 100 m). The dotted and plain white lines represent the*  
 93 *15% and 80% isolines of sea ice cover, respectively, used as lower and upper boundaries of*  
 94 *the Marginal ice zone (MIZ).*

95

96

## 2.2. Hydrography and sea ice cover

97

98

99

100

101

102

103

104

Temperature and salinity profiles were acquired at each of the 60 stations of the cruise using a CTD Sea-Bird SBE 911 Plus. Surface sea-ice concentrations were obtained from daily satellite data (level-2 products at 12.5 km spatial resolution) with the spatial sensor microwave imager (SSM/I). Satellite data for sea ice concentration determination were extracted at each station with the best time and space matching using NASA's SeaDAS image processing software (SeaWiFS Data Analysis System). The freshwater content (FWC) of the upper ocean was calculated to assess the surface water freshening due to sea ice melting and river discharges (McPhee et al., 2009) using the following equation:

$$FWC = \int_{z_{lim}}^0 \left(1 - \frac{S(z)}{S_{ref}}\right) dz$$

105

106

107

108

109

110

111

112

113

114

115

116

where  $S(z)$  is the salinity measured at  $z$  depth,  $S_{ref}$  the reference salinity value, and  $z_{lim}$  the depth at which  $S$  equals  $S_{ref}$ . The latter value is taken at 31, which is the salinity minimum of the Pacific Waters entering the Arctic Ocean through the Bering Strait (Woodgate and Aagaard, 2005). This  $S_{ref}$  value therefore precludes freshening caused by the Pacific Waters inflow and allows estimating the freshening due to sea-ice melting ( $S = 4$ ) and rivers discharge ( $S = 0$ ) only. Overall, the FWC (in m) represents the amount of water needed to account for the negative salinity anomaly relative to 31.

117

118

119

120

121

122

123

To determine the influence of the Beaufort gyre and associated Ekman transport, we calculated the dynamic height  $D$  (in m) between the 0 and 800 m depth. The reference depth of 800 m was chosen to reflect the maximum thickness of the water column affected by Ekman transport. The dynamic height between 0 and 800 m is defined as follows by Thomson and Emery (2001) by:

$$D(0,800) = \int_0^{800} \delta(T, S, p) dp$$

124

125

126

127

$\delta(T, S, p) dp$  is the specific volume anomaly corresponding to the difference between *in situ* density and standard density at the  $p$  depth. The standard density is calculated at a salinity of 35 and of temperature of 0°C.

120 The stratification of the upper layer was estimated by the stratification index ( $\text{kg m}^{-3}$ ),  
121 calculated as the density difference between the surface and 100 m depth (Codispoti et al.,  
122 2005). The polar mixed layer depth (in m) was defined as the depth where density ( $\sigma_t$ )  
123 is  $0.05 \text{ kg m}^{-3}$  higher than the surface density.

124 The euphotic depth was determined using three different methods: satellite data, Secchi disk  
125 measurements and multispectral data of irradiance. The satellite data were obtained from daily  
126 Level 3 Euphotic zone depth products (9 km) of Aqua MODIS ocean color measurements  
127 (<http://oceancolor.gsfc.nasa.gov>) along the CHINARE 2008 ship track with the best time and  
128 space matching using SeaDAS. In the second method, the euphotic depth was calculated as the  
129 depth of 1% of surface light based on Secchi disk measurements in open waters performed on  
130 board. The third estimate of the euphotic depth is the depth corresponding to 1% of surface light  
131 values based on Photosynthetically Available Radiation (PAR) calculated from multispectral data  
132 (Jinping et al., 2010). The three methods provide similar euphotic depth estimates (not shown). In  
133 this study, we used the mean values calculated from these estimates.

### 134 2.3. Nutrients

135 Nutrients were measured at all stations (black and white dots in Fig. 1). Four to 10  
136 depths were sampled in the water column with a minimum of 4 levels in the upper 100 m.  
137 Nutrient concentrations were determined on board using a scan<sup>++</sup> Continuous Flow  
138 AutoAnalyzer (SKALAR). Nitrate concentrations ( $\text{NO}_3^-$ ) were calculated following Wood et  
139 al. (1967). Orthosilicic acid ( $\text{Si(OH)}_4$ ) was measured according to Grasshoff and Ehrhardt  
140 (1983) and phosphate ( $\text{PO}_4^{3-}$ ) as described by Gordon et al. (1993). Primary standards and  
141 reagents were prepared according to the World Ocean Circulation Experiment (WOCE)  
142 protocol. Analytical precision was  $\pm 0.02 \mu\text{M}$  for phosphates and  $\pm 0.1 \mu\text{M}$  for nitrates and  
143 silicates. To determine the nutrient depletion of the surface layer, we calculated the depth of  
144 the nitracline because nitrates are usually the limiting nutrients in the Arctic Ocean (Tremblay  
145 et al., 2006). We identified the shallowest depth layer at which the nitrate gradient is higher  
146 than  $0.1 \mu\text{M m}^{-1}$ . We then calculated the depth of the nitracline as the mid-depth point of this  
147 layer. This parameter indicates the availability of nitrates for primary production.

### 148 2.4. Chlorophyll-*a* and primary production

149 Chlorophyll-*a* concentrations (Chl*a* in  $\text{mg m}^{-3}$ ) were measured at all stations (black and  
150 white dots in Fig. 1) by high-performance liquid chromatography (HPLC) performed at the  
151 Second Institute of Oceanography, Hangzhou, China (SOA) following the method described  
152 in Coupel et al. (2012). The detection limit for Chl*a* is estimated to be  $0.0001 \text{ mg m}^{-3}$ . The  
153 sub-surface chlorophyll maximum (SCM) was determined as the depth of fluorescence

154 maximum based on CTD profiles.

155 *In situ* hourly primary production (PP in  $\text{mg C m}^{-3} \text{ h}^{-1}$ ) was determined at 23 stations (white  
156 dots in Fig. 1). Six depths were sampled based on PAR values at 100%, 50%, 30%, 12%, 5%  
157 and 1% attenuation. The analytical procedure to estimate PP is described by Lee et al. (2010).  
158 Briefly,  $^{13}\text{C}$  isotope-enriched (98–99%)  $\text{H}^{13}\text{CO}_3$  was added to the samples to reach a  
159 concentration of  $\sim 0.2 \mu\text{M } ^{13}\text{CO}_2$  and incubated with running surface seawater. The  $^{13}\text{C}$   
160 enrichment was about 5–10% of the total inorganic carbon in ambient water, as determined by  
161 titration with 0.01N HCl (Anderson et al., 1999). The PP values were linearly interpolated  
162 every meter using the six discrete depth measurements and integrated over the euphotic depth  
163 to calculate the integrated daily PP ( $\text{mg C m}^{-2} \text{ d}^{-1}$ ). The production of carbon by unit Chla  
164 (PP/Chla in  $\text{gC gChla}^{-1} \text{ h}^{-1}$ ) was calculated by dividing hourly PP by the Chla concentration.  
165 A high PP/Chla ratio indicates efficient carbon fixation by phytoplankton while low index  
166 values reflect a poorly efficient carbon fixation.

167

## 168 2.5. Data multivariate analysis

169 Principal component analysis (PCA) is an exploratory statistical method often used to  
170 describe a wide array of individuals and variables (Legendre and Legendre, 2012). When  
171 individuals are described by a large numbers of variables, simple graphical representation of  
172 the correlations existing between variables is not possible. PCA provides a representation in a  
173 lower-dimensional space, defined by eigenvectors, of the maximum variance between data.  
174 Each eigenvector (PC factor) is a linear combination of variables and is associated with a %  
175 of explained variance.

176 In this study, PCA was applied on the normalized dataset to evaluate the correlation between  
177 physical, chemical and environmental variables such as the bathymetry (in m), FWC, depth of  
178 the Pacific Winter Water (PWW), stratification, dynamic height, temperature, sea ice  
179 concentration, polar mixed layer, euphotic depth, nitracline depth and the nitrate  
180 concentrations in the euphotic depth. The following biological variables, PP, surface Chla,  
181 SCM and depth of the SCM, were added as supplementary variables in the analysis.  
182 Eigenvectors of similar and opposite directions indicate positive and negative correlation  
183 between variables, respectively. These multivariate analyses were performed using the ade4  
184 package for R (Chessel et al., 2004).

185

## 186 3. Results

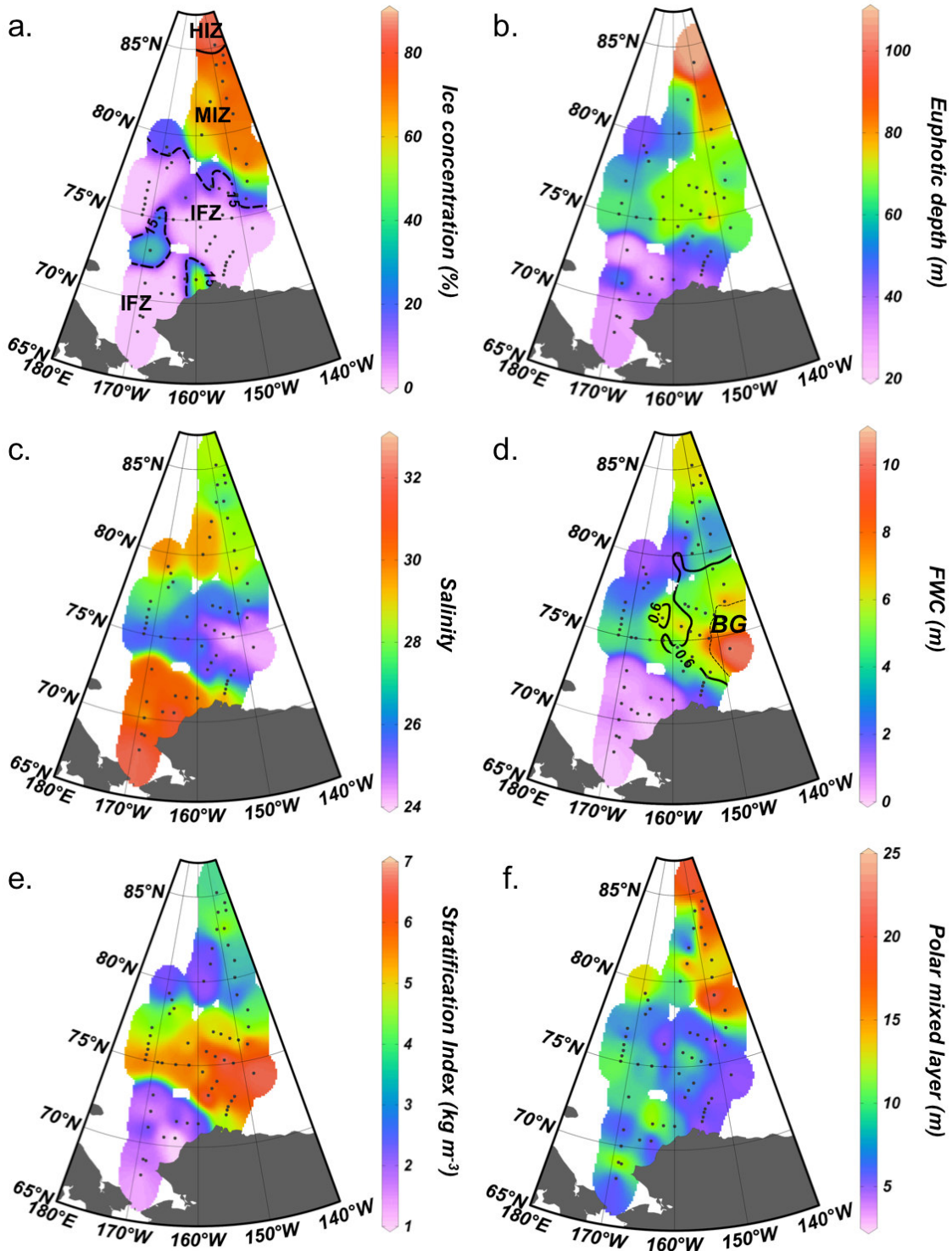
187 **3.1. The physical environment**

188 **3.1.1. Ice cover and euphotic depth**

189 During the CHINARE 2008 cruise, the ice cover in the Pacific Arctic Ocean was  
190 strongly reduced following the minimum multiyear ice coverage on record, in 2007. The  
191 Chukchi shelf was free of ice except for its northern part, which was partially ice-covered  
192 (40% sea ice, Fig. 2a). The ice-free zone (IFZ < 15% of sea ice) was found as far North as  
193 76°N over the Canada Basin in mid-August, and 78°N over the Chukchi Cap, end of August.  
194 The marginal ice zone (MIZ) extended North of the ice-free waters and up to 84°N, in areas  
195 where sea ice cover ranged from 15% to 80%, following the criteria of Strong and Rigor  
196 (2013). The heavy ice zone (HIZ > 80% of sea ice) lied North of 84°N, over the Alpha Ridge.

197 The euphotic depth was two times shallower over the shelf ( $34 \pm 10$  m) than over the  
198 deep basins ( $62 \pm 14$  m; Fig. 2b) and was particularly shallow over the Chukchi Cap and  
199 Mendeleev Abyssal plain region (about 40 m) while deepest (> 80 m) in heavily sea ice  
200 covered areas. However, in sea ice covered areas where satellite data were missing, the  
201 euphotic depth was obtained by the shipside measurements, therefore light penetration does  
202 not account for the effect of the sea ice. However, our light data indicate that these sea ice-  
203 covered waters were the most transparent of the cruise.





204

205 Figure 2. Environmental parameters during the CHINARE cruise in 2008. a. Co-localized sea  
 206 ice concentration obtained from daily spatial sensor microwave imager data (in %). The %  
 207 sea ice is used to distinguish between the ice-free zone (IFZ, ice < 15%), the marginal ice  
 208 zone (MIZ, 15% < ice < 80%) and the heavy ice zone (HIZ, ice > 80%); b. Euphotic depth (in  
 209 m); c. Surface salinity; d. Fresh Water Content (FWC in m). The black line represents the  
 210 dynamic height, indicative of the influence of the Beaufort Gyre (BG). e. Stratification index

211 (in  $\text{kg m}^{-3}$ ); f. Polar mixed layer (in m).  
212

### 213 **3.1.2. Freshening and stratification**

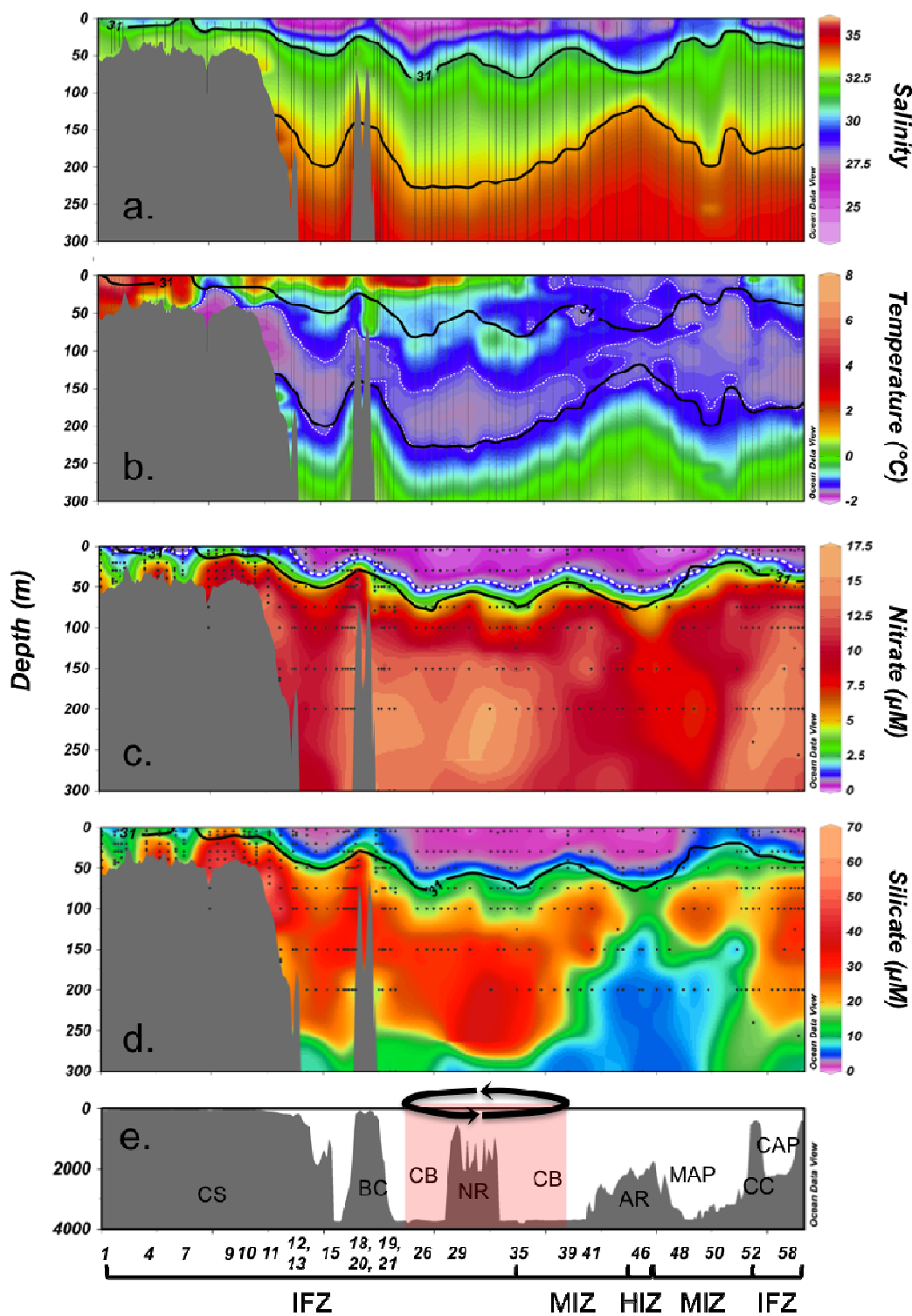
214 In 2008, the freshening and stratification were high and exhibited significant regional  
215 variability. The surface salinity was relatively high over the Chukchi shelf ( $30.7 \pm 0.7$ ; Fig.  
216 2c) compared to the deep basins ( $26.8 \pm 1.7$ ) with surface salinity 2 units lower in the ice-free  
217 basins ( $26.0 \pm 1.4$ ) than in the ice-covered basins. The lowest surface salinity values (24-25)  
218 were found in the southern Canada Basin strongly influenced by the Beaufort Gyre  
219 circulation.

220 The FWC, which provides an integrated view of the freshening, revealed a slightly  
221 different distribution than the surface salinity that reflects primarily surface freshening. The  
222 Chukchi shelf showed the lowest freshwater accumulation (FWC =  $0.4 \pm 0.3$  m; Fig. 2d). i.e.  
223 one order of magnitude lower than over the deep basins. Freshwater strongly accumulates in  
224 the center of Beaufort Gyre (FWC = 5-10 m) and decreases sharply moving away from the  
225 gyre. A FWC value higher than 5 m was also found North of  $83^\circ\text{N}$ , thus far from the Beaufort  
226 Gyre, in a region covered by sea ice. In contrast, the FWC was rather low in the Chukchi Cap  
227 region (FWC = 1-2 m).

228 Stratification tended to be high in areas where surface salinity was low and FWC high.  
229 Indeed, highest stratification was observed in the ice-free deep basins ( $5.5 \pm 0.8 \text{ kg m}^{-3}$ ; Fig.  
230 2e) and peaked in the center of the Beaufort Gyre ( $6-7 \text{ kg m}^{-3}$ ). In contrast, low stratification  
231 was found over the Chukchi shelf ( $1.7 \pm 0.7 \text{ kg m}^{-3}$ ) and in the MIZ ( $3.6 \pm 1 \text{ kg m}^{-3}$ ). The  
232 polar mixed layer was thinner than 25 m in the entire study area (Fig. 2f). In the ice-free  
233 zones, the mixed layer was less than 10 m thick. Surface mixing increased in the ice-covered  
234 deep basins and reached 20 - 25 m when sea ice cover was over 70%.

### 236 **3.2. Water masses and nutrient content**

237 The thickness of the upper ocean layer affected by river discharge and sea ice melting  
238 ( $S < 31$ ) varied regionally, from several meters over the shelf to more than 50 m in the  
239 Beaufort Gyre (Fig. 3a). This freshwater layer exhibited a wide range of temperature from  
240 North to South ( $-1.6$  to  $7^\circ\text{C}$ , Fig. 3b) and a depletion of nitrates ( $\text{NO}_3^- < 2 \mu\text{M}$ , Fig. 3c),  
241 silicates ( $\text{Si} < 5 \mu\text{M}$ , Fig. 3d) and phosphates ( $\text{PO}_4^{3-} < 1 \mu\text{M}$ , not shown).



242

243 **Figure 3.** Vertical sections of the upper 300 m along the CHINARE 2008 ship track. The  
 244 station numbers indicated on the X-axis are those where primary production has been

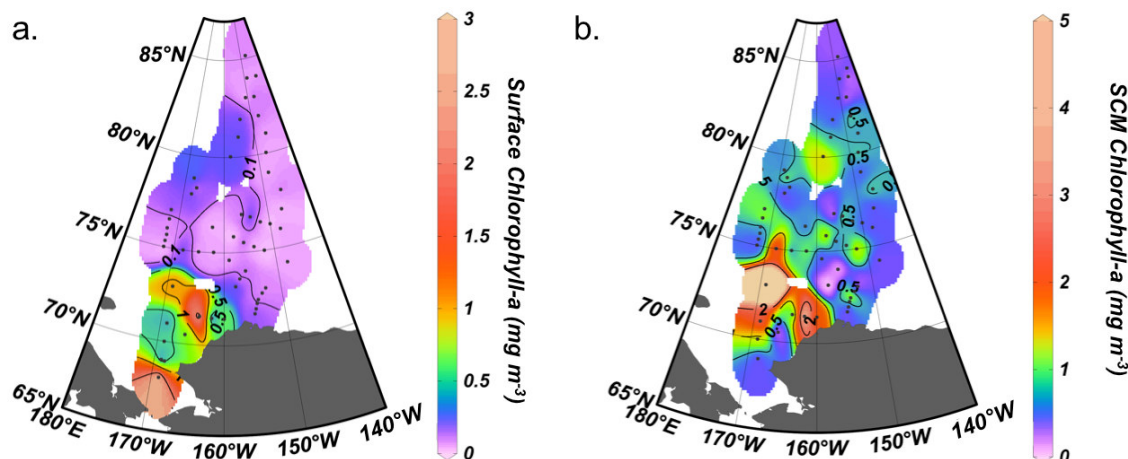
245 measured (white dots in Fig.1). a. salinity; b. temperature (in °C); c. nitrate concentration (in  
 246  $\mu\text{M}$ ), the dotted white line represents the  $1\mu\text{M}$  isoline; d. silicate concentration (in  $\mu\text{M}$ ); e.  
 247 bathymetry (in m). Waters with temperature  $< -1.4^\circ\text{C}$  (dotted white line in panel b) and  
 248 salinity in the range of 31 - 33.5 (black line in panel a and b) are associated with PWW.  
 249 Panel e. indicate the ice conditions (IFZ: Ice free zone; MIZ: Marginal ice zone; HIZ: Heavy  
 250 ice zone) and geographic locations (CS: Chukchi Shelf; BC: Barrow Canyon; CB: Canada  
 251 Basin; NR: Northwind Ridge; AR: Alpha Ridge; MAP: Mendeleev Abyssal Plain; CC:  
 252 Chukchi Cap; CAP: Chukchi Abyssal Plain). The black arrows and overlying red area show  
 253 the region of influence of the Beaufort Gyre.  
 254

255 Freshwater accumulation in the upper layer created a strong salinity gradient from the  
 256 bottom of the mixed layer down to 250 m (Fig. 3a). Nitrate concentration increase with depth  
 257 to reach maximum values at the depth of the Pacific Winter Waters (PWW,  $\text{NO}_3^- > 10 \mu\text{M}$ ,  
 258 Fig. 3c). PWW are usually traced by T values  $< -1.4^\circ\text{C}$ , (Fig. 3b), salinity values lying  
 259 between 31 and 33.5 (Fig. 3a) and a silicate maximum (20-60  $\mu\text{M}$ , Fig. 3d). The nutrient pool  
 260 associated with the PWW was found close to the surface over the Chukchi Shelf (20-50 m)  
 261 and deeper over the basins (100–200 m) (Fig. 3c, 3d). The Pacific Summer Waters (PSW),  
 262 characterized by  $-1.0^\circ\text{C} < T < -0.5^\circ\text{C}$  (between 50 and 100 m; Fig. 3b), had two times lower  
 263 nutrient content than the PWW. The silicate fingerprint of the PWW was observed at all  
 264 stations up to  $85^\circ\text{N}$ , whereas that of the PSW was only observed over the shelf and in the  
 265 southern Canada Basin (Fig. 3d). Thus, during summer the upper Arctic waters were  
 266 characterized by a freshwater layer depleted in nutrients, overlying the sub-surface PWW, the  
 267 major nutrient source for the Arctic basin. The nutrient availability for phytoplankton thus  
 268 depends on physical processes bringing PWW to the surface.  
 269

### 270 3.3. Chlorophyll-*a* and primary production

#### 271 3.3.1. Chlorophyll-*a* concentration

272 Despite a shallow euphotic depth (Fig. 2b), the Chukchi Shelf exhibited the highest  
 273 phytoplankton biomasses observed during the cruise, with mean Chl*a* concentrations of  
 274  $0.88 \pm 0.76 \text{ mg m}^{-3}$  in surface waters (Fig. 4a) and  $1.49 \pm 1.41 \text{ mg m}^{-3}$  in the SCM (Fig. 4b).  
 275 Chl*a* concentration reached a maximum of  $4.94 \text{ mg m}^{-3}$  at 20 m in the Central Canyon (Fig.  
 276 4b). Rather high values,  $2.83 \text{ mg m}^{-3}$  were also observed in surface waters, North of the  
 277 Bering Strait (Fig. 4a). Lowest numbers ( $\sim 0.2 \text{ mg m}^{-3}$ ) were found in shelf waters along the  
 278 Alaskan coast, presumably reflecting the nutrient-depleted waters of the Alaskan Coastal  
 279 Current.



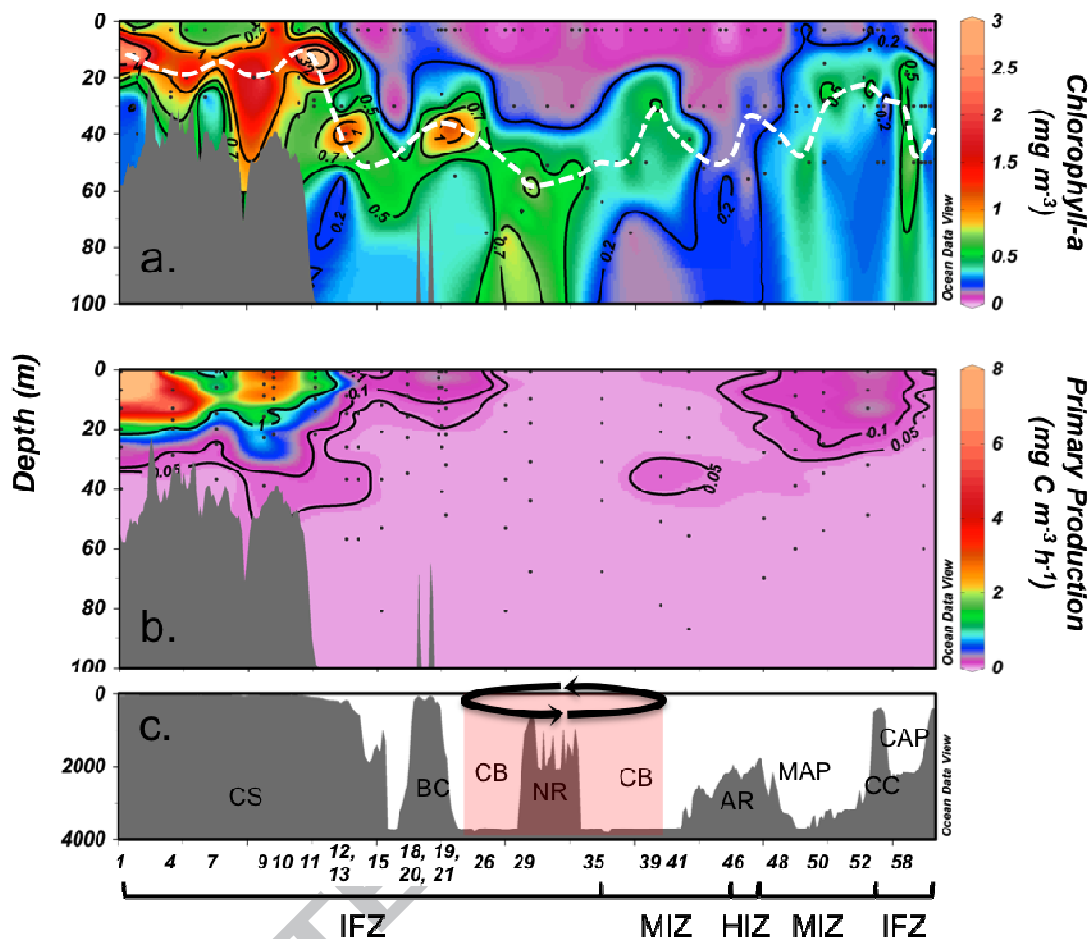
280

281 **Figure 4.** Chlorophyll-*a* concentration in  $\text{mg m}^{-3}$  a. in Surface and b. in the sub-surface  
 282 chlorophyll maximum (SCM).

283

284 Over the deep basins, Chl*a* concentrations were extremely low in surface waters  
 285 ( $0.09 \pm 0.08 \text{ mg m}^{-3}$ , Fig. 4a, 5a) but relatively high in the SCM ( $0.42 \pm 0.28 \text{ mg m}^{-3}$ , Fig. 4b,  
 286 5a) compared to mean values found in the oligotrophic subtropical gyre waters ( $\sim 0.1 \text{ mg m}^{-3}$ ,  
 287 (Sarmiento and Gruber, 2006)). Chl*a* concentrations in the SCM of the basin were highly  
 288 variable, ranging from  $0.05 \text{ mg Chl a m}^{-3}$  over the Alpha Ridge to  $1.43 \text{ mg Chl a m}^{-3}$  at the  
 289 mouth of Barrow Canyon. Surface Chl*a* at some stations of the continental slope and over the  
 290 Chukchi Cap - Mendeleev Abyssal Plain region were quite remarkable with concentrations 2  
 291 to 5 times higher than found at other stations of the deep basin.

292 The depth of the SCM varied regionally (Fig. 5a). The SCM depth was, on average 2  
 293 times deeper over the basins ( $47 \pm 17 \text{ m}$ ) than over the Chukchi shelf ( $24 \pm 8 \text{ m}$ ). The SCM  
 294 was deeper in the Canada Basin ( $53 \pm 13 \text{ m}$ ), on the northern transit in August, than in the  
 295 Mendeleev Abyssal Plain, Chukchi Cap and Chukchi Abyssal Plain ( $38 \pm 11 \text{ m}$ ), occupied on  
 296 the way back, in early September. The SCM was about shallower at the edge of the Beaufort  
 297 Gyre than in the ice-free regions of the Canada Basin. Finally, offshore Central Canyon and  
 298 Barrow Canyon the SCM was relatively deep (about 40 m) with a high Chl*a* content ( $> 1 \text{ mg}$   
 299  $\text{m}^{-3}$ ).



300 **Figure 5.** Vertical sections of the upper 100 m showing a. Chlorophyll-a (in  $\text{mg m}^{-3}$ ) and the  
 301 depth of the subsurface Chla maximum (white dashed line); b. Primary production ( $\text{mg C m}^{-3}$   
 302  $\text{h}^{-1}$ ); c. bathymetry from the surface to 4000 m depth (in m). The stations where primary  
 303 production was measured (white dots in Fig.1) are indicated on the X-axis. Panel c. gives the  
 304 ice conditions (IFZ: Ice free zone; MIZ: Marginal ice zone; HIZ: Heavy ice zone) and  
 305 geographic locations (CS: Chukchi Shelf; BC: Barrow Canyon; CB: Canada Basin; NR:  
 306 Northwind Ridge; AR: Alpha Ridge; MAP: Mendeleev Abyssal Plain; CC: Chukchi Cap;  
 307 CAP: Chukchi Abyssal Plain). The black arrows and red shaded area highlight the Beaufort  
 308 Gyre.  
 309

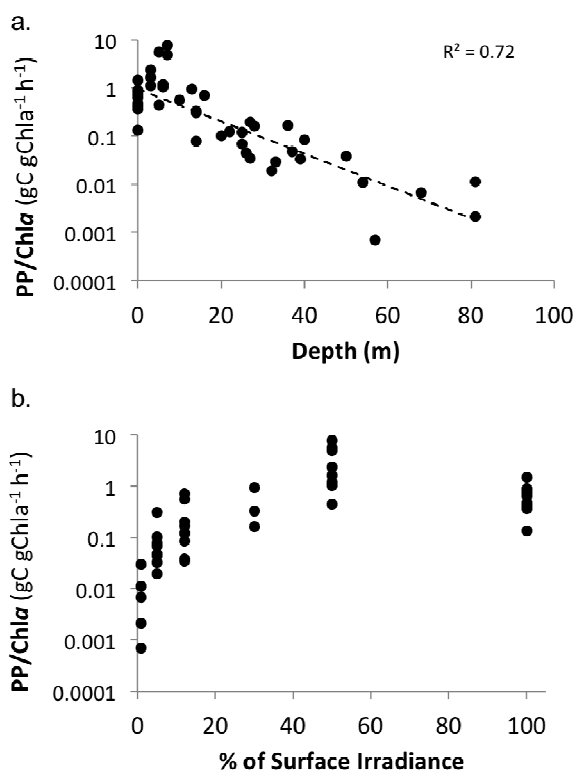
310

311 

### 3.3.2. Primary production

312 The highest PP levels were found in the upper 20 m of the Chukchi Shelf, with values  
 313 ranging from  $0.4 \text{ mg C m}^{-3} \text{ h}^{-1}$ , near the Alaskan coast, to  $19.6 \text{ mg C m}^{-3} \text{ h}^{-1}$ , near Bering  
 314 Strait, with an average value of  $2.0 \pm 2.1 \text{ mg C m}^{-3} \text{ h}^{-1}$  in the euphotic depth layer (Fig. 5b).  
 315 Over the deep basins, PP was one to two orders of magnitude lower. The Mendeleev Abyssal  
 316 Plain/Chukchi Cap and the Barrow Canyon regions had the highest PP of the deep basin ( $0.2$

317  $\pm 0.01 \text{ mg C m}^{-3} \text{ h}^{-1}$ ). In contrast, the Canada Basin and Alpha Ridge regions showed the  
 318 lowest PP ( $< 0.1 \text{ mg C m}^{-3} \text{ h}^{-1}$ ). Our results also show that the PP/Chla ratio decrease  
 319 exponentially with depth (Fig. 6a). Phytoplanktonic communities in the upper 10 m produce  
 320 100 times more C per unit of Chla, than those living at 60 m. The highest PP/Chla ratios (1 to  
 321 10) were observed at the depth receiving 50% of the surface irradiance (Fig. 6b). At 5% and  
 322 1% of surface irradiance, productivity is 100 to 1000 times lower than at 50%. Note that the  
 323 PP/Chla ratios were one order of magnitude lower in surface waters (100% of surface  
 324 irradiance) than at 50 % irradiance depth, suggesting light inhibition of surface  
 325 phytoplanktonic communities.



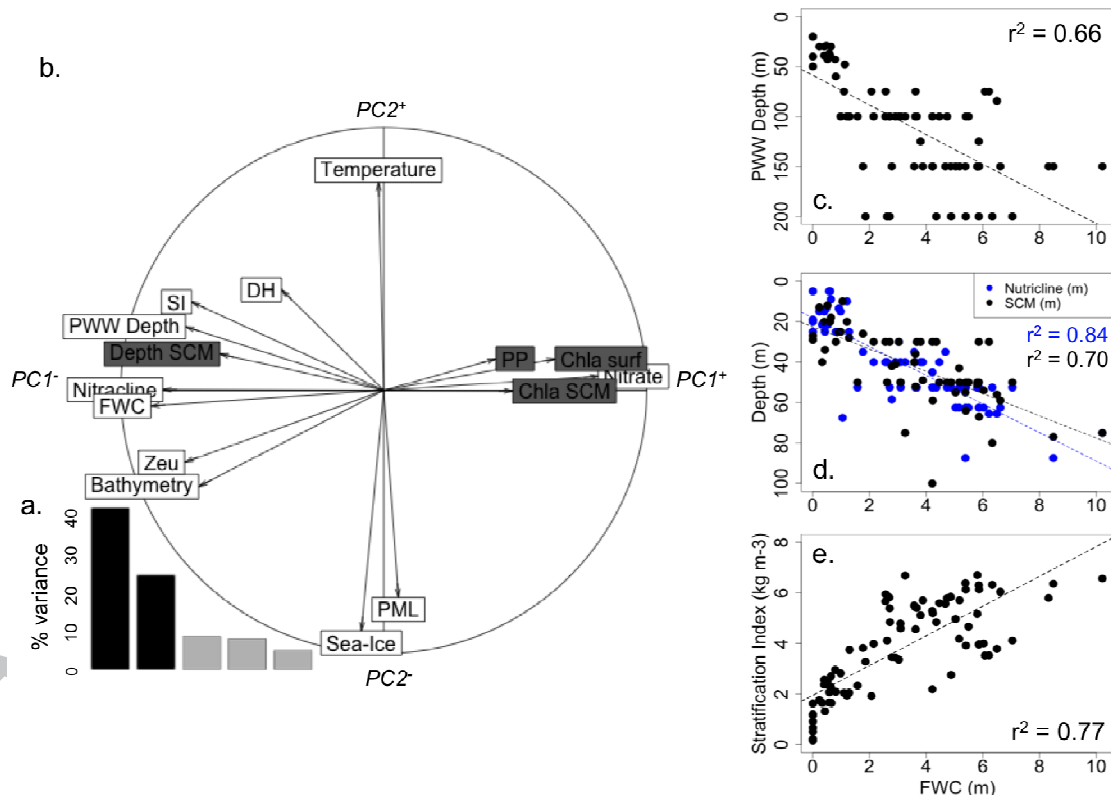
326  
 327 **Figure 6.** PP/Chla ratio values plotted as a function of **a.** depth (in m) and **b.** percentage of  
 328 surface irradiance. Note that the Y-axis is in log scale.

329

### 330 3.4. Principal component analysis

331 Figures 7a and 7b show the result of the PCA performed on our dataset (60 stations and 15  
 332 variables). The two first axes of the PCA explain more than 65% of the total variance (Fig.  
 333 7a). Bathymetry, FWC, PWW depth, nitracline, nitrate concentration, stratification, euphotic  
 334 depth and dynamic height are the main variables responsible for the construction of PC1  
 335 whereas temperature, sea ice concentration and polar mixed layer primarily account for the

336 construction of PC2 (Fig. 7b). The PCA results also reveal that the bathymetry, FWC,  
 337 euphotic depth (Zeu), nitracline depth, PWW depth, the dynamic height and stratification  
 338 index were positively correlated (PC1<sup>-</sup>) while these variables were negatively correlated with  
 339 nitrate concentrations (PC1<sup>+</sup>). The PC2 shows that the surface temperature (PC2<sup>+</sup>) was  
 340 negatively correlated with the sea ice concentration and the PML depth (PC2<sup>-</sup>). Moreover, the  
 341 PCA indicates that temperature, sea ice concentration and polar mixed layer depth were  
 342 independent of the variables linked to PC1. The over plot of biological parameters (PP, Chla  
 343 surf, Chla SCM, SCM depth) added as supplementary variables, suggest that higher PP and  
 344 Chla concentrations are associated with shallower SCM. Biological variables do not seem to  
 345 be influenced by variables accounting for PC2.  
 346 These results underline the correlations between FWC and PWW depth (Fig 7c), the FCW  
 347 and the nitracline and SCM depth (Fig 7d), and between the FCW and stratification index (Fig  
 348 7e).  
 349



350

351 **Figure 7:** Results of the Principal component analysis (PCA) of the CHINARE 2008 dataset  
 352 a. Percentage of explained variance of each of the five first PC axes. Black bars indicate the  
 353 variance explained by the two first axis; b. PCA factor loadings plot; White labels correspond  
 354 to active variables in the calculations, while dark grey labels are the added biological  
 355 variables, not used for the calculations. PML: Polar Mixed Layer; Sea-Ice: sea ice cover;



356 *FWC: Fresh Water Content; Zeu: euphotic zone depth; DH: Dynamic Height; PWW depth:*  
357 *depth of the Pacific Winter Water; SI: stratification index; Nitracline: depth of the nitracline;*  
358 *Bathymetry: bottom depth; Nitrate: mean nitrate concentration over the euphotic depth;*  
359 *Depth SCM: depth of the sub-surface chlorophyll maximum; Chla surf: chlorophyll-a*  
360 *concentration in surface waters; Chla SCM: chlorophyll-a concentration in the sub-surface*  
361 *chlorophyll maximum; PP: Primary Production integrated over the euphotic depth; c. FWC*  
362 *versus PWW depths; d. FWC versus the nitracline depths (blue dots) and FWC versus SCM*  
363 *depths (black dots); e. FWC versus SI. The determination coefficient corresponding to the*  
364 *linear fit of each sub-dataset is also shown.*  
365

## 366 **4. Discussion**

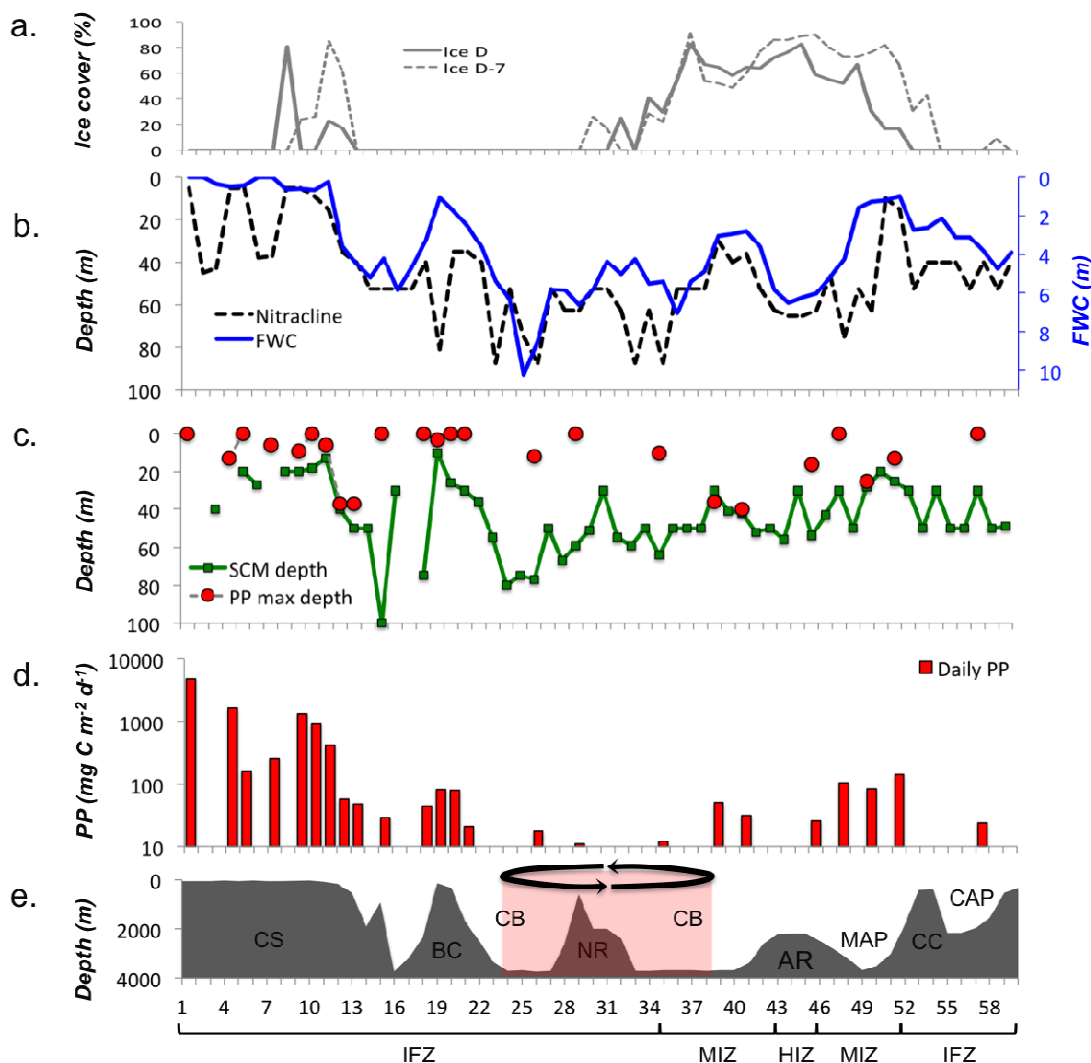
### 367 **4.1. The freshening as a control of the nutrient availability**

368 The multivariate method PCA is used here to discuss the relationship between variables  
369 presumably important to phytoplankton production. As can be seen from Figure 7b, PP and  
370 Chla concentrations were not directly affected by either sea ice concentration or the  
371 temperature and depth of the mixed layer, as reflected by the orthogonal direction of PC1 and  
372 PC2. This supports the idea that phytoplankton was not light-limited in summer 2008 in  
373 contrast to icy years when offshore phytoplankton was restrained by a shallow light  
374 penetration (Gosselin et al., 1997; Hill and Cota, 2005). We observed that most of the Pacific  
375 sector of the Arctic Ocean was free of ice and that the euphotic depth was deeper than the  
376 mixed layer. Satellite data indicate that 2008 was the year of minimum multiyear ice coverage  
377 on record (Maslanik et al., 2011) in agreement with *in situ* sea-ice observations during the  
378 cruise showing prevailing first-year ice and the omnipresence of melt ponds (Lu et al., 2010).  
379 Given that first-year sea ice transmits 3-fold more light than multiyear sea ice (Frey et al.,  
380 2011; Nicolaus et al., 2012), it is likely that the light penetration was also high in waters  
381 covered by sea ice (MIZ and HIZ). The high transparency of sea ice covered waters (Fig. 2b)  
382 may have favored light transmission in the water column.

383 The PCA shows that the highest PP and Chla concentrations were related to high nitrate  
384 concentrations and a shallow nitracline. This relationship highlights that under reduced sea ice  
385 cover, PP would be primarily controlled by nutrient availability in the euphotic layer as  
386 reported by several studies (Tremblay and Gagnon, 2009; Tremblay et al., 2002; Tremblay et  
387 al., 2006). The nutrient-rich regions with high PP and Chla were observed at low FWC, weak  
388 stratification, deep PWW and both shallow euphotic layer and bathymetry. In contrast,  
389 nutrient-poor regions with low PP and Chla were associated with high FWC, strong  
390 stratification, shallow PWW and both deep euphotic layer and bathymetry. We suggest that a  
391 high FWC, resulting from increased thickness of the freshwater surface layer, deepened the  
392 sub-surface nutrients reservoir of PWW (Fig. 7c) and strengthened stratification (Fig. 7e).

393 Such stratified conditions then reduce vertical mixing and subsequently the renewal of  
394 nutrients from PWW. Consequently, regions with high FWC exhibit stronger surface water  
395 nitrate depletion and a deeper nitracline and SCM (Fig. 7d). Moreover, the nitrate depletion of  
396 the surface layer may be enhanced by the low nutrient content of sea-ice meltwater. Melnikov  
397 et al. (2002) reported mean summer silicate and phosphate concentrations in sea ice that are  
398 below 1 and 0.5  $\mu\text{M}$ , respectively. The observed impact of freshening on the nitracline and  
399 SCM depth is consistent with earlier observations in the Canada Basin, between 2002 and  
400 2009, and confirm the effect of freshening on PP and Chl*a*, as hypothesized by McLaughlin  
401 and Carmack (2010).

402 The negative impact of FWC on primary production appeared to be linked to the influence  
403 of the nitracline depth on the SCM. Despite relatively high Chl*a* concentrations, deep SCM  
404 exhibit very low rates of carbon fixation as shown by the exponential decrease of the PP/Chl*a*  
405 ratio with depth (Fig. 6a). In fact, the deep communities under light-limited conditions need to  
406 produce more Chl*a* to absorb light. This is illustrated by the depth difference between the  
407 SCM and PP maximum. The more productive stations (Fig. 8d) had shallow nitraclines (Fig.  
408 8b) and SCM depths close or associated with the PP maximum (Fig. 8c). Conversely, poorly  
409 productive stations coincide with a deep nitracline and much deeper SCMs than the PP  
410 maximum. This was particularly true for the southern Canada Basin where, due to the  
411 influence of the Beaufort Gyre on nitracline depth, the SCM was deeper than 60 m while  
412 maximum PP was found at approximately 15 m.



413

414 **Figure 8.** Environmental and biological parameters from the different provinces measured at  
 415 the 60 stations of the CHINARE 2008 cruise (Fig. 1). a. Ice cover (%) measured the day of  
 416 sampling, *D* (grey thick line) and 7 days prior to sampling, *D*-7 (grey dashed line); b. Depth  
 417 of the nitracline (in m) (black dashed line) and of the Fresh Water Content (in m) (FWC, blue  
 418 line); c. Depth of the chlorophyll maximum (in m) (SCM, green line) and of the maximum PP  
 419 rates (red dots); d. Daily primary production integrated over the euphotic depth (PP in mg C  
 420  $m^{-2} d^{-1}$ ); e. Bathymetry (in m) with the ice conditions (IFZ: Ice free zone; MIZ: Marginal ice  
 421 zone; HIZ: Heavy ice zone) and geographic locations, CS: Chukchi Shelf; BC: Barrow  
 422 Canyon; CB: Canada Basin; NR: Northwind Ridge; AR: Alpha Ridge; MAP: Mendeleev  
 423 Abyssal Plain; CC: Chukchi Cap; CAP: Chukchi Abyssal Plain. The black arrows and  
 424 overlying red area show the region influenced by the Beaufort Gyre.  
 425

426

#### 4.2. Freshwater drives the regional productivity

427

428

Since freshening appears to be a controlling factor of nutrient availability, PP and Chl<sub>a</sub>  
 concentrations, its spatial distribution and regional impact were investigated across the study

429 area. Although the FWC distribution is thought to reflect sea ice cover and melting, high  
430 FWC was found in heavily ice-covered regions, and lower FWC in the ice-free Chukchi shelf  
431 (Fig. 8a, 8b). In fact, a large fraction of the freshwater input to the upper Arctic Ocean is of  
432 riverine origin (Jones et al., 2008). This amount of freshwater is redistributed by the ocean  
433 circulation (i.e. the Pacific inflow, the Beaufort Gyre spin up and the transpolar drift) leading  
434 to regional differences of the FWC depth (Giles et al., 2012; Morison et al., 2012). In the  
435 following, we investigate regional causes of FWC and its impact on primary producers.

#### 436 **4.2.1. Intense freshening in the ice-free basins reinforces oligotrophy**

437 The ice-free southern Canada Basin was the region most affected by freshening due to  
438 influenced of the Beaufort Gyre circulation. Stronger freshening led to thinnest mixed layer (<  
439 10 m), strongest stratification ( $> 5 \text{ kg m}^{-3}$ ) and deepest PWW nutrient pool (about 150 m,  
440 Table 1). The Beaufort Gyre region was characterized by a marked nitrate depletion down to  
441 60 m (Fig. 3c, 3d) and a deep SCM ( $59 \pm 16 \text{ m}$ ) (Fig. 8c). The very low PP/Chl*a* ratios at the  
442 SCM ( $0.01 \pm 0.01 \text{ g C gChl}^{-1} \text{ h}^{-1}$ , Table 1) point out slow-growing communities and their  
443 adaptation to reduced light intensity rather than active production of carbon biomass. The  
444 integrated PP values over the ice-free Canada Basin ( $24 \pm 15 \text{ mg C m}^{-2} \text{ d}^{-1}$ , Table 1) were 3 to  
445 5 times lower than those found in the same area in August 1993, when the region was covered  
446 by sea-ice and less affected by freshening ( $123 \text{ mg C m}^{-2} \text{ d}^{-1}$  (Cota et al., 1996)) or in July  
447 2005 ( $60 \text{ mg C m}^{-2} \text{ d}^{-1}$  (Lee et al., 2010)). These features may, in part, also reflect seasonal  
448 effects. Indeed, the earlier sea-ice retreat in recent years could explain earlier nutrient  
449 depletion and subsequent lower primary production rates at this time of the year.

450 The ice-free Chukchi Abyssal Plain was also associated with a strong stratification and  
451 weak vertical mixing driving low surface water Chl*a* concentration ( $0.09 \pm 0.07 \text{ mg Chl} \text{ m}^{-3}$ ,  
452 Table 1). The weaker influence of the Beaufort Gyre was likely responsible for lower FWC  
453 ( $3.2 \pm 0.8 \text{ m}$ ) and a 15 m shallower nitracline and SCM than found in the southern Canada  
454 Basin. However, the Chukchi Abyssal Plain waters were sampled 2 weeks after those of the  
455 Canada Basin, allowing for more nutrient consumption by phytoplankton. The PP values in  
456 this area ( $24 \text{ mg C m}^{-2} \text{ d}^{-1}$ ) were similar as those of the ice-free Canada Basin but the PP/Chl*a*  
457 ratio was slightly higher, emphasizing better carbon fixation efficiency by primary producers.  
458 The large dominance of nanoplankton in these two poorly-productive ice-free basins (Coupel  
459 et al., 2012) support earlier observations of Li et al. (2009) showing that small cell algae  
460 flourish as the Arctic Ocean freshens.

461

462 **Table 1:** The mean values of physical and biogeochemical parameters are presented for the  
 463 stations located over the shelf (depth < 100m) and over deep basins (depth > 100m). Sub-  
 464 provinces of the basin are clustered according to geographical location and sea-ice  
 465 conditions, i.e. the ice-free zone (IFZ, ice < 15%); the marginal ice zone (MIZ, 15% < ice  
 466 < 80%) and the heavy ice zone (HIZ, ice > 80%). The Chukchi Shelf, Canada Basin and Alpha  
 467 Ridge were visited in August 2008 while the Chukchi Abyssal Plain, the Chukchi Cap (CC)  
 468 and the Mendeleev Abyssal Plain (MAP) were visited during the way back, in September.  
 469 FWC: Freshwater Content; SI: Stratification Index; the Pacific Winter Water (PWW) depth is  
 470 determined with three criteria:  $T < -0.5^{\circ}\text{C}$ ;  $31 < S < 33.5$ ;  $PP_{eu}$  is the daily primary  
 471 production integrated over the euphotic depth. The ratio  $PP/Chla$  is given for surface waters  
 472 and subsurface Chlorophyll a maximum (SCM).  
 473

	Ice cover (%)	FWC (m)	SI ( $\text{kg m}^{-3}$ )	PWW depth (m)	Nitracline (m)	SCM depth (m)	Chlorophyll a ( $\text{mg m}^{-3}$ )		$PP_{eu}$ ( $\text{mg C m}^{-2} \text{d}^{-1}$ )	$PP/Chla$ ( $\text{gC gChla}^{-1} \text{h}^{-1}$ )	
							Surface	SCM		Surface	SCM
<b>SHELF</b> (n = 11) (z < 100m)	6 ± 15	0.4 ± 0.3	1.7 ± 0.6	39 ± 11	22 ± 15	24 ± 8	0.88 ± 0.76	1.49 ± 1.41	1380 ± 1628	3.6 ± 2.7	0.2 ± 0.2
<b>BASIN</b> (n = 49) (z > 100m)	22 ± 31	4.3 ± 2.0	4.4 ± 1.9	134 ± 39	53 ± 17	47 ± 17	0.09 ± 0.08	0.45 ± 0.34	51 ± 37	0.8 ± 0.5	0.06 ± 0.06
<b>IFZ</b> (74-78°N) (Canada Basin)	2 ± 5	5.5 ± 1.8	5.9 ± 0.6	150 ± 30	59 ± 16	55 ± 17	0.08 ± 0.07	0.47 ± 0.39	24 ± 15	0.6 ± 0.2	0.01 ± 0.01
<b>IFZ</b> (75-78°N) (Chukchi Abyssal Plain)	0 ± 0	3.2 ± 0.8	4.9 ± 0.7	134 ± 44	45 ± 6	42 ± 10	0.09 ± 0.07	0.44 ± 0.23	24	0.8	0.03
<b>MIZ</b> (78-83°N) (Canada Basin)	56 ± 23	4.5 ± 1.5	4.0 ± 1.0	136 ± 52	52 ± 17	48 ± 9	0.05 ± 0.03	0.39 ± 0.15	32 ± 19	0.5 ± 0.2	0.08 ± 0.08
<b>MIZ</b> (78-83°N) (CC +MAP)	46 ± 24	2.4 ± 1.8	2.6 ± 0.8	100 ± 0	43 ± 26	33 ± 11	0.20 ± 0.11	0.55 ± 0.28	111 ± 29	0.7 ± 0.3	0.15 ± 0.04
<b>HIZ</b> (83-86°N) (Alpha Ridge)	78 ± 8	6.1 ± 0.3	3.8 ± 0.2	95 ± 27	64 ± 2	47 ± 12	0.05 ± 0.01	0.22 ± 0.11	26	0.4	0.02

474

475

#### 4.2.2. Heavily ice-covered basins also affected by freshening

476

477

478

479

480

481

482

483

484

485

486

487

488

489

490

High freshening was also observed in the heavily ice covered Alpha Ridge zone (HIZ, Table 1). Freshwater at such high latitudes result from sea-ice meltwater and water discharges from the Siberian Rivers as previously reported (Johnson and Polyakov, 2001; Jones et al., 2008; Semiletov et al., 2000; Serreze et al., 2006). Enhanced freshening is associated with a nutrient depleted layer as deep as  $64 \pm 2$  m. However, it is difficult to disentangle the effect of freshening and phytoplankton consumption. Considering the high transparency of the waters (Fig. 2b) and the presence of first-year ice and melt ponds (Lu et al., 2010), nutrients may have been consumed by phytoplankton as deep as 64 m. Although biomasses are very low at the surface ( $0.05 \pm 0.05 \text{ mg Chla m}^{-3}$ ) and in the SCM ( $0.22 \pm 0.11 \text{ mg Chla m}^{-3}$ ), the only available integrated PP at these high latitudes ( $26 \text{ mg C m}^{-2} \text{d}^{-1}$ ) indicate values close to those found in the ice-free basins. Note that sea ice algae were not considered and therefore primary production is likely be underestimated. Nevertheless, nutrient depletion at such high latitudes could also be a permanent feature due to low mixing rates, amplified by summer freshening. Another possible explanation for low primary production, is the limited northern expansion of nutrient-rich PWW over the Alpha Ridge zone, resulting in 3 times lower silicate and nitrate

491 concentrations in the subsurface layer than found in the southern basin (Fig. 3c, 3d).

#### 492 **4.2.3. Enhanced productivity in regions with low freshening**

493 The highest PP values in the deep basins ( $111 \pm 29 \text{ mg C m}^{-2} \text{ d}^{-1}$ ) were found in the  
494 MIZ over the Mendeleev Abyssal Plain characterized by the lowest FWC. At these stations,  
495 surface and SCM Chla were highest (Table 1). The SCM were relatively shallow and  
496 occurred at the same depth than PP maxima (Fig. 8c). The phytoplankton in the SCM was 20  
497 times more efficient in carbon fixation ( $\text{PP/Chla} = 0.15 \pm 0.04 \text{ gC gChla}^{-1} \text{ h}^{-1}$ ) than in the ice-  
498 free and heavy ice-covered regions. High abundances of penate diatoms *Nitzschia sp.* and  
499 *Fragilariopsis sp.* in this area (Coupel et al., 2012) indicate that new production was  
500 stimulated by high light and nutrient availability.

501 Lower freshening in the MIZ could result from the interaction between wind and ice-  
502 edge, promoting vertical mixing and upwelling of nutrient-rich deep waters (Mundy et al.,  
503 2009; Tremblay and Gagnon, 2009; Tremblay et al., 2011), and a weak stratification (Fig. 2e,  
504 Table 1). In addition, the sea ice data show that the Mendeleev Abyssal Plain experienced a  
505 50% decrease in sea ice cover during the preceding week (ice D-7 in Fig. 8a), allowing for  
506 increasing light penetration and phytoplankton to reach a “new” pool of nutrients. Enrichment  
507 in the MIZ is usually observed over the continental shelf but can extend over the deep basins  
508 as sea ice melting proceeds during the summer season. However, production and biomass in  
509 the offshore MIZ remained one order of magnitude lower than typical spring ice edge blooms  
510 over the Arctic shelves (Niebauer and Alexander, 1985).

511 Enhanced PP was less clear in the MIZ of the Canada Basin, with values 3 times lower  
512 than in the MIZ of the Mendeleev Abyssal Plain. The higher initial FWC and deeper PWW  
513 nutrient reservoir caused by the Beaufort Gyre circulation could explain the lower  
514 phytoplankton growth in the MIZ of the Canada Basin. Although reduced vertical mixing  
515 could have prevented replenishment from the deeper nutrient reservoir, we cannot rule out  
516 earlier nutrient consumption by phytoplankton. Indeed, two weeks prior the station  
517 occupation, sea ice had receded in the MIZ of the Canada Basin providing favorable  
518 conditions for phytoplankton growth. Nevertheless, we found relatively high PP values at  
519 stations 39 ( $32 \text{ mg C m}^{-2} \text{ d}^{-1}$ ) and 41 ( $51 \text{ mg C m}^{-2} \text{ d}^{-1}$ ), while sea ice cover was on the order  
520 of 60% (Fig. 8d). Owing to their position at the edge of the Beaufort Gyre, FWC was lower at  
521 the northern sites than in the southern Canada Basin. Lower FWC was associated with a  
522 shallower nitracline and SCM (Fig 8b), the latter coinciding with the PP maximum depth (Fig.  
523 8c). Our results also indicate that phytoplanktonic communities in the SCM were as efficient  
524 to fix carbon ( $\text{PP/Chla} = 0.12 \pm 0.06 \text{ gC gChla}^{-1} \text{ h}^{-1}$ ) as those of the MIZ over the Mendeleev

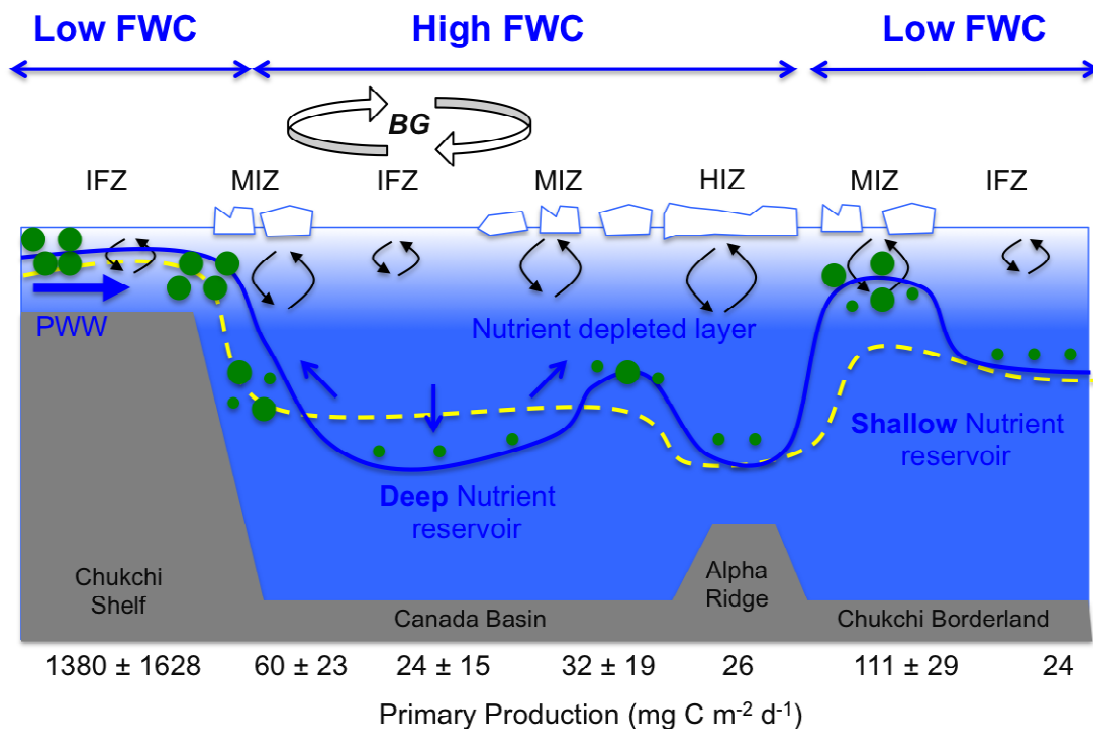
525 Abyssal Plain.

#### 526 **4.2.4. A productive shelf weakly affected by the freshening**

527 The FWC was generally low over the shelf, presumably, because of the short residence  
528 time of shelf waters (Weingartner et al., 2005; Woodgate et al., 2005). Low FWC and weak  
529 stratification favor the replenishment of nutrients from the deeper water layer and surface  
530 sediments. The Pacific waters entering through Bering strait is another source of nutrient  
531 supply (Sambrotto et al., 1984; Springer and McRoy, 1993). The high PP and biomass of  
532 surface waters in the southern Chukchi shelf support the hypothesis of a nutrient supply from  
533 Bering Strait even in late summer. While highest PP values were found in the southern shelf  
534 waters, highest biomasses were encountered in the SCM of the northern shelf waters (close to  
535  $5 \text{ mg Chl}a \text{ m}^{-3}$ , Fig. 4b). The low temperature ( $T < -1^\circ\text{C}$ ) (Fig. 3b) and high silicate content of  
536 the surface waters of the northern shelf ( $\text{Si} > 50 \mu\text{M}$ ) (Fig. 3d) suggest that biomass  
537 production could have been promoted by upwelling cells due to the retreat of the ice cover  
538 from 80% to less than 20% in one week (Fig. 8a). Biomasses and integrated PP over the  
539 Chukchi shelf in 2008 ( $1469 \pm 2040 \text{ mg C m}^{-2} \text{ d}^{-1}$ , Table 1) were within the range of previous  
540 summer season data over the Chukchi shelf ( $170\text{--}1940 \text{ mg C m}^{-2} \text{ d}^{-1}$  (Hameedi, 1978);  $500\text{--}$   
541  $4700 \text{ mg C m}^{-2} \text{ d}^{-1}$  (Springer and McRoy, 1993);  $750 \text{ mg C m}^{-2} \text{ d}^{-1}$  (Cota et al., 1996);  
542  $2570 \text{ mg C m}^{-2} \text{ d}^{-1}$ , (Gosselin et al., 1997);  $780 \text{ mg C m}^{-2} \text{ d}^{-1}$ , (Hill and Cota, 2005);  $1000 \text{ mg}$   
543  $\text{C m}^{-2} \text{ d}^{-1}$ , (Tremblay et al., 2012)). These values were also close to those reported in the MIZ  
544 of the central Barents Sea ( $500\text{--}1400 \text{ mg C m}^{-2} \text{ d}^{-1}$  (Reigstad et al., 2002)). The fact that our  
545 data are within the range of previous observations indicates that the recent freshening of the  
546 Arctic Ocean does not significantly affect the Chukchi shelf water primary production.  
547 Nevertheless, the comparison with earlier studies should be considered with caution because  
548 of the high spatial and temporal variability of primary production in the region, the difference  
549 in sampling period and changes in the phenology of Arctic ecosystems (Melnikov and  
550 Kolosova, 2001).

#### 551 **4.3. Towards an increase or decrease of primary production in Arctic?**

552 Our results reveal that phytoplankton biomass and primary production in summer were  
553 primarily controlled by freshening and sea ice conditions. While sea ice can stimulates  
554 phytoplankton growth by modifying light availability, freshening acts on the nutrient reservoir  
555 and its replenishment from deeper waters. The combined effect of sea ice and freshening on  
556 the nutrient availability and primary producers is conceptualized in Figure 9.



557

558 **Figure 9:** Conceptual model showing the nutrient and light availability in regions differently  
 559 affected by sea-ice (IFZ, MIZ and HIZ), the freshening of the upper layer (Low and High) and  
 560 the Beaufort Gyre circulation (BG). The blue line represents the nitracline that distinguishes  
 561 the nutrient-depleted upper layer, from the subsurface Pacific Winter Water (PWW) nutrient  
 562 reservoir. The dashed yellow line indicates the euphotic zone depth. The green dots sketch the  
 563 phytoplankton biomass. The black arrows are indicative of surface mixing. Integrated  
 564 primary production (PP) mean values (mg C m<sup>-2</sup> d<sup>-1</sup>) are given for each oceanographic  
 565 provinces at the bottom of the figure.

566

567 High FWC depicts conditions encountered in the Canada Basin, while low FWC were  
 568 observed over the Chukchi Borderland (Chukchi Abyssal Plain, Chukchi Cap and Mendeleev  
 569 Abyssal Plain) and Chukchi Shelf. In the low freshening scenario, sea ice retreat over the deep  
 570 basins is prone to create « hot spots » because of a shallower nutrient reservoir and a weaker  
 571 stratification. These « hot spots » for primary production in the summer of 2008 occurred  
 572 mainly in the MIZ over the Chukchi Borderland, with a mean integrated daily PP value (111 ±  
 573 29 mg C m<sup>-2</sup> d<sup>-1</sup>) that was larger than those observed in August 1994 in the same area under  
 574 heavily ice-covered (9–73 mg C m<sup>-2</sup> d<sup>-1</sup> (Gosselin et al. 1997)). In contrast, in the Canada  
 575 Basin, where freshening was high and largely due to the Beaufort Gyre, phytoplankton growth  
 576 in the MIZ was four times weaker. Because of a deeper nutrient reservoir and a stronger  
 577 stratification, more energy is required to bring deep nutrients to the surface.

578 Under ice-free conditions, wind forcing can promote the deepening of the mixed layer and



579 therefore nutrient depletion of the upper layer (Rainville et al., 2011). Longer ice-free  
580 conditions during autumn also contribute to favor vertical mixing by winds. Yet, ice-free  
581 basins were most strongly nutrient depleted. Stronger winds will thus be needed for deeper  
582 nutrient-rich layer to replenish surface waters. Nutrient depletion reached deeper layers in the  
583 ice-free Canada Basin than in the ice-free Chukchi Abyssal Plain because of higher  
584 freshening. Consequently, phytoplankton communities developed deeper in the ice-free  
585 Canada basin and displayed lowest carbon production values because of nutrient limitations.  
586 In the context of global warming, ice melting and freshening of the Arctic Ocean is predicted  
587 to intensify in the future (Peterson et al., 2006; Yamamoto-Kawai et al., 2009). The  
588 subsequent environment changes in this polar region are likely to have strong implication on  
589 the marine ecosystem, in particular in the deep basins.

590

## 591 **5. Conclusion**

592 Primary production and chlorophyll-*a* vertical distributions in the Pacific sector of the  
593 Arctic Ocean in summer 2008 were tightly linked to the FWC in the upper surface layer.  
594 Regions strongly affected by freshening, such as ice-free basins (73°-77°N) and heavily ice-  
595 covered areas (83°-86°N) displayed the lowest PP, lowest surface Chl*a* (nutrient limitation)  
596 and a deep and weakly productive sub-surface chlorophyll-*a* maximum (nutrient and light  
597 limitations). In contrast, "hot spots", with 2 to 5 times higher Chl*a* and PP values than  
598 generally found in the deep basins, were observed across the offshore marginal ice zone  
599 (MIZ) over the Chukchi Borderland (77°- 82°N). The recent break-up of sea ice at the higher  
600 most latitudes allowed phytoplankton to thrive on the nutrient deeper pool. These transition  
601 zones between ice-covered and ice-free waters experienced lower FWC and nutrient  
602 replenishment of surface waters from the underlying Pacific waters. Nevertheless, stimulation  
603 of the primary producers of the MIZ was not significant in the Canada Basin, more affected  
604 by the freshening than the Chukchi Borderland due to Beaufort Gyre. Similarly, the ice-free  
605 Canada Basin experienced a 15 m deeper nutrient depletion than the ice-free Chukchi Abyssal  
606 Plain, less affected by the Beaufort Gyre. The Chukchi shelf, with the lower FWC, was the  
607 most productive area of the cruise with biomasses and primary production values in the range  
608 of those reported in previous summer studies in that area. The highest Chl*a* values in the  
609 northern shelf were associated to upwelling cells of nutrient-rich waters at the shelf break  
610 while the highest PP observed in the south were sustained by nutrient-rich Pacific waters  
611 entering the Bering Strait.

612 While ice cover seems to play a key role in triggering phytoplankton growth, the FWC

613 appears to be a crucial factor of the phytoplankton response to summer sea ice retreat, by  
614 acting on the nutrient reservoir depth. Overall, our results suggest that in the context of future  
615 global warming, the reduction of nutrient availability due to increase FWC could counteract  
616 the expected phytoplankton response to sea ice retreat, i.e. an increase of biomass and PP due  
617 to enhanced light penetration and a longer growing season.

618

#### 619 **Acknowledgements**

620 This research is a contribution to the Arctic Tipping Points (ATP) project (<http://www.eu-atp.org>) funded by FP7  
621 of the European Union (contract #226248) and the European program DAMOCLES (Developing Arctic  
622 Modeling and Observing Capabilities for Long-term Environmental Studies, 2007–2010) and Chinese IPY  
623 program/National Natural Science Foundation of China (No. 41076135). Support for Lee was provided by the  
624 Korea Research Foundation (KRF) grant funded by the Korea government (MEST) (No. 2011-0007761). We  
625 express our gratitude to the captain and the crew of the Chinese icebreaker *Xuelong* for the opportunity to take  
626 part in the fieldwork in the Arctic Ocean. We thank Chinese Arctic and Antarctic Administration extending an  
627 invitation to French scientists from the LOCEAN laboratory (UPMC – Université de Pierre et Marie Curie) to  
628 participate in the CHINARE cruise. We especially thank the SIOSOA (Hangzhou, China) for supporting the stay  
629 of French scientists in their laboratory and the pigment analysis (by HPLC), as well as their warm welcome and  
630 helpfulness. We are grateful to Mr S. Q. Gao, Y. Lu and Ms. H. Jin (SIO-SOA, Hangzhou, China) for their help  
631 in the nutrient analysis and sample collection, as well as professor J.P. Zhao (Ocean University China, Qingdao,  
632 China) and the Chinese and Finnish physical teams (Finnish Meteorological Institute, Helsinki) for the  
633 acquisition and transfer of the hydrological data (CTD). Philippe Lattes is warmly thanked for his help in the  
634 creation of several computer programs used to interpret the data.

635

#### 636 **References**

- 637 Anderson, L. G., Jones, E. P., and Rudels, B.: Ventilation of the Arctic Ocean estimated by a plume entrainment  
638 model constrained by CFCs, *Journal of Geophysical Research-Oceans*, 104, 13423-13429, 1999.
- 639 Anderson, L. G., Tanhua, T., Björk, G., Hjalmarsson, S., Jones, E. P., Jutterström, S., Rudels, B., Swift, J. H.,  
640 and Wählström, I.: Arctic ocean shelf–basin interaction: An active continental shelf CO<sub>2</sub> pump and its impact on  
641 the degree of calcium carbonate solubility, *Deep Sea Research Part I: Oceanographic Research Papers*, 57, 869-  
642 879, 2010.
- 643 Ardyna, M., Gosselin, M., Michel, C., Poulin, M., and Tremblay, J. E.: Environmental forcing of phytoplankton  
644 community structure and function in the Canadian High Arctic: contrasting oligotrophic and eutrophic regions,  
645 *Marine Ecology Progress Series*, 442, 37-57, 2011.
- 646 Arrigo, K. R., van Dijken, G., and Pabi, S.: Impact of a shrinking Arctic ice cover on marine primary production,  
647 *Geophysical Research Letters*, 35, L19603, 2008.
- 648 Bates, N. R., Moran, S. B., Hansell, D. A., and Mathis, J. T.: An increasing CO<sub>2</sub> sink in the Arctic Ocean due to  
649 sea-ice loss, *Geophysical Research Letters*, 33, L23609, 2006.
- 650 Cai, W. J., Chen, L., Chen, B., Gao, Z., Lee, S. H., Chen, J., Pierrot, D., Sullivan, K., Wang, Y., Hu, X., Huang,  
651 W. J., Zhang, Y., Xu, S., Murata, A., Grebeiner, J. M., Jones, E. P., and Zhang, H.: Decrease in the CO<sub>2</sub> uptake  
652 capacity in an ice-free Arctic Ocean basin, *Science*, 329, 556-559, 2010.
- 653 Carmack, E. and Chapman, D. C.: Wind-driven shelf/basin exchange on an Arctic shelf: The joint roles of ice  
654 cover extent and shelf-break bathymetry, *Geophysical Research Letters*, 30, 1778, 2003.
- 655 Carmack, E. and Wassmann, P.: Food webs and physical–biological coupling on pan-Arctic shelves: Unifying  
656 concepts and comprehensive perspectives, *Progress in Oceanography*, 71, 446-477, 2006.
- 657 Chessel, D., Dufour, A. B., and Thioulouse, J.: The ade4 package-I-One-table methods, *R news*, 4, 5-10, 2004.
- 658 Codispoti, L. A., Flagg, C., Kelly, V., and Swift, J. H.: Hydrographic conditions during the 2002 SBI process

- 659 experiments, *Deep-Sea Res Pt II*, 52, 3199-3226, 2005.
- 660 Comiso, J. C., Parkinson, C. L., Gersten, R., and Stock, L.: Accelerated decline in the Arctic sea ice cover,  
661 *Geophysical Research Letters*, 35, L01703, 2008.
- 662 Cota, G. F., Pomeroy, L. R., Harrison, W. G., Jones, E. P., Peters, F., Sheldon, W. M., and Weingartner, T. R.:  
663 Nutrients, primary production and microbial heterotrophy in the southeastern Chukchi Sea: Arctic summer  
664 nutrient depletion and heterotrophy, *Marine Ecology Progress Series*, 135, 247-258, 1996.
- 665 Coupel, P., Jin, H. Y., Joo, M., Horner, R., Bouvet, H. A., Sicre, M. A., Gascard, J. C., Chen, J. F., Garçon, V.,  
666 and Ruiz-Pino, D.: Phytoplankton distribution in unusually low sea ice cover over the Pacific Arctic,  
667 *Biogeosciences*, 9, 4835-4850, 2012.
- 668 Frey, K. E., Perovich, D. K., and Light, B.: The spatial distribution of solar radiation under a melting Arctic sea  
669 ice cover, *Geophysical Research Letters*, 38, L22501, 2011.
- 670 Giles, K. A., Laxon, S. W., Ridout, A. L., Wingham, D. J., and Bacon, S.: Western Arctic Ocean freshwater  
671 storage increased by wind-driven spin-up of the Beaufort Gyre, *Nature Geoscience*, 5, 194-197, 2012.
- 672 Gordon, L. I., Jennings Jr, J. C., Ross, A. A., and Krest, J. M.: A suggested protocol for continuous flow  
673 automated analysis of seawater nutrients (phosphate, nitrate, nitrite and silicic acid) in the WOCE Hydrographic  
674 Program and the Joint Global Ocean Fluxes Study, *WOCE Operations Manual, Part, 3*, 91-91, 1993.
- 675 Gosselin, M., Levasseur, M., Wheeler, P. A., Horner, R. A., and Booth, B. C.: New measurements of  
676 phytoplankton and ice algal production in the Arctic Ocean, *Deep Sea Research Part II: Topical Studies in  
677 Oceanography*, 44, 1623-1644, 1997.
- 678 Grasshoff, K. and Ehrhardt, M.: *K. Kremling (1983): Methods of Seawater Analysis*. Weinheim: Verlag Chemie,  
679 1983.
- 680 Hameedi, M. J.: Aspects of water column primary productivity in the Chukchi Sea during summer, *Marine  
681 Biology*, 48, 37-46, 1978.
- 682 Hill, V. and Cota, G.: Spatial patterns of primary production on the shelf, slope and basin of the Western Arctic  
683 in 2002, *Deep Sea Research Part II: Topical Studies in Oceanography*, 52, 3344-3354, 2005.
- 684 Jinping, Z., Weibo, W., and Lee, C.: Calculation of photosynthetically available radiation using multispectral  
685 data in the Arctic, *Chinese Journal of Polar Research*, 2, 2010.
- 686 Johnson, M. A. and Polyakov, I. V.: The Laptev Sea as a source for recent Arctic Ocean salinity changes,  
687 *Geophysical Research Letters*, 28, 2017-2020, 2001.
- 688 Jones, E. P., Anderson, L. G., Jutterström, S., Mintrop, L., and Swift, J. H.: Pacific freshwater, river water and  
689 sea ice meltwater across Arctic Ocean basins: Results from the 2005 Beringia Expedition, *Journal of  
690 Geophysical Research*, 113, C08012, 2008.
- 691 Lee, S., Stockwell, D., and Whittleage, T.: Uptake rates of dissolved inorganic carbon and nitrogen by under-ice  
692 phytoplankton in the Canada Basin in summer 2005, *Polar Biology*, 33, 1027-1036, 2010.
- 693 Lee, S. H. and Whittleage, T. E.: Primary and new production in the deep Canada Basin during summer 2002,  
694 *Polar Biology*, 28, 190-197, 2004.
- 695 Legendre, P. and Legendre, L.: *Numerical ecology*, Elsevier, 2012.
- 696 Li, W. K., McLaughlin, F. A., Lovejoy, C., and Carmack, E. C.: Smallest algae thrive as the Arctic Ocean  
697 freshens, *Science*, 326, 539, 2009.
- 698 Longhurst, A. R.: Role of the Marine Biosphere in the Global Carbon-Cycle, *Limnology and Oceanography*, 36,  
699 1507-1526, 1991.
- 700 Lu, P., Li, Z., Cheng, B., Lei, R., and Zhang, R.: Sea ice surface features in Arctic summer 2008: Aerial  
701 observations, *Remote Sensing of Environment*, 114, 693-699, 2010.
- 702 Maslanik, J., Stroeve, J., Fowler, C., and Emery, W.: Distribution and trends in Arctic sea ice age through spring  
703 2011, *Geophysical Research Letters*, 38, L13502, 2011.
- 704 Mauritzen, C.: Oceanography Arctic Freshwater, *Nature Geoscience*, 5, 162-164, 2012.
- 705 McLaughlin, F. A. and Carmack, E. C.: Deepening of the nutricline and chlorophyll maximum in the Canada  
706 Basin interior, 2003–2009, *Geophysical Research Letters*, 37, L24602, 2010.
- 707 McPhee, M. G., Proshutinsky, A., Morison, J. H., Steele, M., and Alkire, M. B.: Rapid change in freshwater  
708 content of the Arctic Ocean, *Geophysical Research Letters*, 36, L10602, 2009.
- 709 Melnikov, I. and Kolosova, E.: The Canada Basin zooplankton in recent environmental changes in the Arctic  
710 Ocean, *Proceedings of the Arctic Regional Centre, "Changes in the atmosphere-land-sea system in the Amerasian  
711 Arctic*, 3, 165-176, 2001.
- 712 Morison, J., Kwok, R., Peralta-Ferriz, C., Alkire, M., Rigor, I., Andersen, R., and Steele, M.: Changing Arctic  
713 Ocean freshwater pathways, *Nature*, 481, 66-70, 2012.
- 714 Mundy, C. J., Gosselin, M., Ehn, J., Gratton, Y., Rossnagel, A., Barber, D. G., Martin, J., Tremblay, J.-É.,  
715 Palmer, M., Arrigo, K. R., Darnis, G., Fortier, L., Else, B., and Papakyriakou, T.: Contribution of under-ice  
716 primary production to an ice-edge upwelling phytoplankton bloom in the Canadian Beaufort Sea, *Geophysical  
717 Research Letters*, 36, L17601, 2009.
- 718 Nicolaus, M., Katlein, C., Maslanik, J., and Hendricks, S.: Changes in Arctic sea ice result in increasing light

- 719 transmittance and absorption, *Geophysical Research Letters*, 39, 2012.
- 720 Niebauer, H. J. and Alexander, V.: Oceanographic Frontal Structure and Biological Production at an Ice Edge,  
721 *Continental Shelf Research*, 4, 367-388, 1985.
- 722 Pabi, S., van Dijken, G. L., and Arrigo, K. R.: Primary production in the Arctic Ocean, 1998–2006, *Journal of*  
723 *Geophysical Research*, 113, 2008.
- 724 Perovich, D. K.: The Changing Arctic Sea Ice Cover, *Oceanography*, 24, 162-173, 2011.
- 725 Perovich, D. K., Richter-Menge, J. A., Jones, K. F., and Light, B.: Sunlight, water, and ice: Extreme Arctic sea  
726 ice melt during the summer of 2007, *Geophysical Research Letters*, 35, L11501, 2008.
- 727 Peterson, B. J., McClelland, J., Curry, R., Holmes, R. M., Walsh, J. E., and Aagaard, K.: Trajectory shifts in the  
728 Arctic and subarctic freshwater cycle, *Science*, 313, 1061-1066, 2006.
- 729 Poulin, M., Daugbjerg, N., Gradinger, R., Ilyash, L., Ratkova, T., and Quillfeldt, C.: The pan-Arctic biodiversity  
730 of marine pelagic and sea-ice unicellular eukaryotes: a first-attempt assessment, *Marine Biodiversity*, 41, 13-28,  
731 2010.
- 732 Rabe, B., Karcher, M., Schauer, U., Toole, J. M., Krishfield, R. A., Pisarev, S., Kauker, F., Gerdes, R., and  
733 Kikuchi, T.: An assessment of Arctic Ocean freshwater content changes from the 1990s to the 2006–2008  
734 period, *Deep Sea Research Part I: Oceanographic Research Papers*, 58, 173-185, 2011.
- 735 Rainville, L., Lee, C., and Woodgate, R.: Impact of Wind-Driven Mixing in the Arctic Ocean, *Oceanography*,  
736 24, 136-145, 2011.
- 737 Reigstad, M., Wassmann, P., Wexels Riser, C., Øygarden, S., and Rey, F.: Variations in hydrography, nutrients  
738 and chlorophyll a in the marginal ice-zone and the central Barents Sea, *Journal of Marine Systems*, 38, 9-29,  
739 2002.
- 740 Sambrotto, R. N., Goering, J. J., and McRoy, C. P.: Large yearly production of phytoplankton in the Western  
741 bering strait, *Science*, 225, 1147-1150, 1984.
- 742 Sarmiento, J. L. and Gruber, N.: *Ocean biogeochemical dynamics*, Princeton University Press Princeton, 2006.
- 743 Semiletov, I., Savelieva, N., Weller, G., Pipko, I., Pugach, S., Gukov, A. Y., and Vasilevskaya, L.: The  
744 dispersion of Siberian river flows into coastal waters: Meteorological, hydrological and hydrochemical aspects.  
745 In: *The freshwater budget of the Arctic Ocean*, Springer, 2000.
- 746 Serreze, M. C., Barrett, A. P., Slater, A. G., Woodgate, R. A., Aagaard, K., Lammers, R. B., Steele, M., Moritz,  
747 R., Meredith, M., and Lee, C. M.: The large-scale freshwater cycle of the Arctic, *Journal of Geophysical*  
748 *Research*, 111, C11010, 2006.
- 749 Springer, A. M. and McRoy, C. P.: The paradox of pelagic food webs in the northern Bering Sea—III. Patterns  
750 of primary production, *Continental Shelf Research*, 13, 575-599, 1993.
- 751 Stroeve, J. C., Serreze, M. C., Holland, M. M., Kay, J. E., Malanik, J., and Barrett, A. P.: The Arctic's rapidly  
752 shrinking sea ice cover: a research synthesis, *Climatic Change*, 110, 1005-1027, 2011.
- 753 Strong, C. and Rigor, I. G.: Arctic marginal ice zone trending wider in summer and narrower in winter,  
754 *Geophysical Research Letters*, 40, 4864-4868, 2013.
- 755 Thomson, R. E. and Emery, W. J.: *Data analysis methods in physical oceanography*, Elsevier, 2001.
- 756 Tremblay, J.-É. and Gagnon, J.: The effects of irradiance and nutrient supply on the productivity of Arctic  
757 waters: a perspective on climate change, *Nato Sci Peace Secur*, doi: 10.1007/978-1-4020-9460-6\_7, 2009. 73-93,  
758 2009.
- 759 Tremblay, J. E., Belanger, S., Barber, D. G., Asplin, M., Martin, J., Darnis, G., Fortier, L., Gratton, Y., Link, H.,  
760 Archambault, P., Sallon, A., Michel, C., Williams, W. J., Philippe, B., and Gosselin, M.: Climate forcing  
761 multiplies biological productivity in the coastal Arctic Ocean, *Geophysical Research Letters*, 38, L18604, 2011.
- 762 Tremblay, J. E., Gratton, Y., Fauchot, J., and Price, N. M.: Climatic and oceanic forcing of new, net, and diatom  
763 production in the North Water, *Deep-Sea Res Pt II*, 49, 4927-4946, 2002.
- 764 Tremblay, J. E., Michel, C., Hobson, K. A., Gosselin, M., and Price, N. M.: Bloom dynamics in early opening  
765 waters of the Arctic Ocean, *Limnology and Oceanography*, 51, 900-912, 2006.
- 766 Tremblay, J. E., Robert, D., Varela, D. E., Lovejoy, C., Darnis, G., Nelson, R. J., and Sastri, A. R.: Current state  
767 and trends in Canadian Arctic marine ecosystems: I. Primary production, *Climatic Change*, 115, 161-178, 2012.
- 768 Wassmann, P. and Reigstad, M.: Future Arctic Ocean Seasonal Ice Zones and Implications for Pelagic-Benthic  
769 Coupling, *Oceanography*, 24, 220-231, 2011.
- 770 Weingartner, T., Aagaard, K., Woodgate, R., Danielson, S., Sasaki, Y., and Cavalieri, D.: Circulation on the  
771 north central Chukchi Sea shelf, *Deep Sea Research Part II: Topical Studies in Oceanography*, 52, 3150-3174,  
772 2005.
- 773 Wood, E. D., Armstrong, F. A., and Richards, F. A.: Determination of Nitrate in Sea Water by Cadmium-Copper  
774 Reduction to Nitrite, *Journal of the Marine Biological Association of the United Kingdom*, 47, 23-31, 1967.
- 775 Woodgate, R. A. and Aagaard, K.: Revising the Bering Strait freshwater flux into the Arctic Ocean, *Geophysical*  
776 *Research Letters*, 32, L02602, 2005.
- 777 Woodgate, R. A., Aagaard, K., and Weingartner, T. J.: A year in the physical oceanography of the Chukchi Sea:  
778 Moored measurements from autumn 1990–1991, *Deep Sea Research Part II: Topical Studies in Oceanography*,

779 52, 3116-3149, 2005.  
780 Yamamoto-Kawai, M., McLaughlin, F. A., Carmack, E. C., Nishino, S., Shimada, K., and Kurita, N.: Surface  
781 freshening of the Canada Basin, 2003–2007: River runoff versus sea ice meltwater, *Journal of Geophysical*  
782 *Research*, 114, C00A05, 2009.  
783 Yun, M. S., Whitledge, T. E., Kong, M., and Lee, S. H.: Low primary production in the Chukchi Sea shelf, 2009,  
784 *Continental Shelf Research*, 76, 1-11, 2014.  
785 Zhang, J., Ashjian, C., Campbell, R., Hill, V., Spitz, Y. H., and Steele, M.: The great 2012 Arctic Ocean summer  
786 cyclone enhanced biological productivity on the shelves, *Journal of Geophysical Research: Oceans*, 119, 297-  
787 312, 2014.  
788  
789

ACCEPTED MANUSCRIPT

- The freshwater content (FWC) appears to be a crucial factor of the phytoplankton response to summer sea ice retreat, by acting on the nutrient reservoir depth.
- The strong freshening observed in the Canada Basin had a negative impact on primary producers.
- Biomasses accumulation and relatively high primary production were observed across the offshore marginal ice zone.
- The Chukchi shelf, with the lower FWC, was the most productive area of the cruise with biomasses and primary production values in the range of previous studies.